UNIVERSITÄT AUGSBURG
Universitätsbibliothek

OPEN ACCESS
OPUS AUGSBURG

Electronic and vibrational properties of the low-dimensional perovskites Sr1−yLayNbO3.5−x

Christine A. Kuntscher, S. Schuppler, P. Haas, B. P. Gorshunov, Martin Dressel, M. Grioni, Frank Lichtenberg

Angaben zur Veröffentlichung / Publication details:

Kuntscher, Christine A., S. Schuppler, P. Haas, B. P. Gorshunov, Martin Dressel, M. Grioni, and Frank Lichtenberg. 2004. "Electronic and vibrational properties of the low-dimensional perovskites Sr1−yLayNbO3.5−x." *Physical Review B* 70 (24): 245123. https://doi.org/10.1103/physrevb.70.245123.

Nutzungsbedingungen / Terms of use:

licgercopyright

Dieses Dokument wird unter folgenden Bedingungen zur Verfügung gestellt: / This document is made available under these conditions:
Deutsches Urheberrecht
Weitere Informationen finden Sie unter: / For more information see:
https://www.uni-augsburg.de/de/organisation/bibliothek/publizieren-zitieren-archivieren/publiz/

Electronic and vibrational properties of the low-dimensional perovskites $Sr_{1-y}La_yNbO_{3.5-x}$

C. A. Kuntscher
Forschungszentrum Karlsruhe, Institut für Festkörperphysik, D-76021 Karlsruhe, Germany and 1. Physikalisches Institut, Universität Stuttgart, Pfaffenwaldring 57, D-70550 Stuttgart, Germany

S. Schuppler
Forschungszentrum Karlsruhe, Institut für Festkörperphysik, D-76021 Karlsruhe, Germany

P. Haas, B. Gorshunov,* and M. Dressel
1. Physikalisches Institut, Universität Stuttgart, Pfaffenwaldring 57, D-70550 Stuttgart, Germany

M. Grioni
Institut de Physique Appliquée, Ecole Polytechnique Fédérale, CH-1015 Lausanne, Switzerland

F. Lichtenberg
Experimentalphysik VI, Institut für Physik, EKM, Universität Augsburg, Universitätsstrasse 1, D-86135 Augsburg, Germany
(Received 25 May 2004; revised manuscript received 27 August 2004; published 27 December 2004)

By angle-resolved photoemission spectroscopy and polarization-dependent infrared reflectivity measurements the electronic and vibrational properties of the low-dimensional perovskites $Sr_{1-y}La_yNbO_{3.5-x}$ were studied along different crystal directions. The electronic behavior strongly depends on the oxygen and La content, including quasi-one-dimensional metallic and ferroelectric insulating behavior. An extremely small energy gap at the Fermi level is found for $SrNbO_{3.41}$ and $SrNbO_{3.45}$ along the conducting direction at low temperature, suggestive for a Peierls-type instability. Despite the similar nominal carrier density, for $Sr_{0.8}La_{0.2}NbO_{3.50}$ the quasi-one-dimensional metallic character is suppressed and no gap opening is observed, which can be explained by differences in the crystal structure. Electron-phonon interaction appears to play an important role in this series of compounds.

DOI: 10.1103/PhysRevB.70.245123 PACS number(s): 71.10.Pm, 71.20.Ps, 79.60.−i, 78.20.Ci

I. INTRODUCTION

The observation of quasi-one-dimensional (quasi-1D) metallic behavior of some members of the perovskite-related series $Sr_{1-y}La_yNbO_{3.5-x}$, with $0 \leqslant x \leqslant 0.1$, raised interest recently.[1,2] It comprises compounds with a wide range of electronic properties,[3] including a ferroelectric insulator, semiconducting compounds, and quasi-1D metals. They have an orthorhombic, perovskite-related crystal structure with lattice parameters $a \approx 3.9$ Å, $b \approx 5.5$ Å, and c depending on the oxygen content,[3–5] and belong to the homologous series of the type $Sr_nNb_nO_{3n+2}$. The main building blocks of the structure are NbO_6 octahedra, which are grouped into slabs extending along the (a,b) plane. The width of the slabs along c is determined by the oxygen content and directly given by the parameter n: While for quasi-1D metallic $SrNbO_{3.40}$ ($n=5$) the slabs are five octahedra wide, ferroelectric, insulating $SrNbO_{3.50}$ ($n=4$) consists of four octahedra wide slabs. For defined oxygen stoichiometries in the range $0 \leqslant x \leqslant 0.1$ the structure exhibits a well-ordered stacking sequence of the ($n=5$) and ($n=4$) subunits, listed in Table I for the investigated compounds.[3,5,6] A schematic drawing of the idealized crystal structure of three representative $SrNbO_{3.50-x}$ compounds is shown in Fig. 1. The real crystal structure exhibits a considerable distortion of the NbO_6 octahedra, with different magnitude depending on the position within the slab. Along the a axis the octahedra are connected continuously via the apical oxygen sites forming 1D chains, as is illustrated in Ref. 2. The oxygen content not only determines the crystal structure but also the number of Nb 4d conduction electrons. A second doping channel which, however, does not affect the width and stacking sequence of the slabs is the substitution of divalent Sr by a higher-valent element like La. The nominal numbers of Nb 4d conduction electrons per formula unit for the present niobates, derived within an ionic picture, are listed in Table I.

According to dc resistivity measurements, the electronic properties of $SrNbO_{3.41}$ and $Sr_{0.8}La_{0.2}NbO_{3.50}$ are highly anisotropic, with lowest, metal-like resistivity values along the

TABLE I. Studied niobates of the type $Sr_nNb_nO_{3n+2}$. For each composition the stacking sequence of the ($n=5$) and ($n=4$) subunits per unit cell and the nominal number z of Nb 4d conduction electrons per formula unit are given.

	Stacking sequence	z
$SrNbO_{3.41}$	-5-5-5-5-	0.18
$SrNbO_{3.45}$	-4-5-4-5-	0.1
$SrNbO_{3.50}$	-4-4-4-4-	0
$Sr_{0.8}La_{0.2}NbO_{3.50}$	-4-4-4-4-	0.2
$Sr_{0.7}Ba_{0.1}La_{0.2}NbO_{3.50}$	-4-4-4-4-	0.2
$Sr_{0.6}Ca_{0.2}La_{0.2}NbO_{3.50}$	-4-4-4-4-	0.2

 ©2004 The American Physical Society

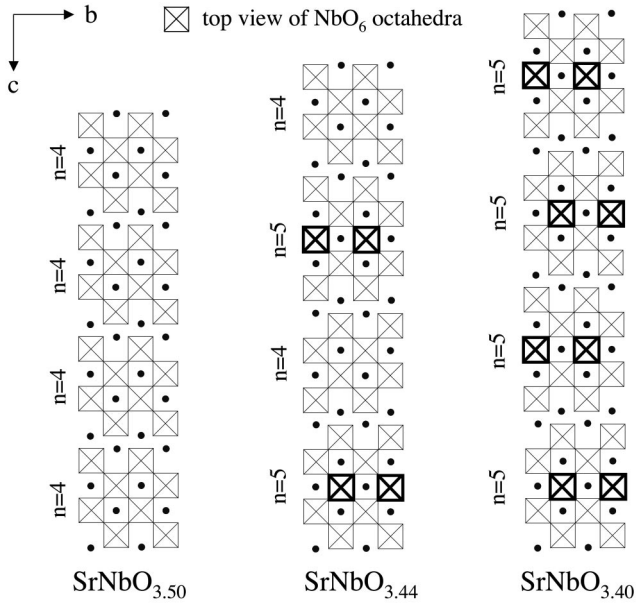

FIG. 1. Schematic drawing of the idealized, i.e., nondistorted, crystal structures of three compounds of the series $Sr_nNb_nO_{3n+2}$. The NbO_6 units in the middle of the slabs, which presumably are the conducting channels of the lattice, are marked by thick lines.

a direction.[3] The temperature dependence of the resistivity along the *a* axis, ρ_a, consists of several regimes; taking $SrNbO_{3.41}$ as an example, one observes the following behavior. Starting from the lowest temperature, the resistivity decreases strongly, showing a minimum around 50 K and increases between 50 and $\approx$130 K. Above $\approx$130 K ρ_a decreases slightly with increasing temperature. The resistivity behavior below 50 K can be described by an activated behavior $\rho \propto \exp[E_a/(k_BT)]$ with activation energies $E_a = 2-3$ meV.[2,3] An explanation for the temperature behavior of ρ_a above 50 K is so far missing. A similar temperature dependence is observed for $Sr_{0.8}La_{0.2}NbO_{3.50}$.

On the other hand, $SrNbO_{3.50}$ ($n=4$) is a band insulator. It is ferroelectric below $T_c = 1613$ K with a spontaneous polarization along the *b* axis.[7,8] The compound undergoes two further phase transitions, namely a second-order phase transition to an incommensurate phase at 488 K and another ferroelectric transition at 117 K with an additional component of the spontaneous polarization appearing along the *c* axis.[9]

The magnetic properties of the investigated niobium oxide compounds were described in Ref. 3. Except $SrNbO_{3.50}$, all compounds show a similar behavior. With increasing temperature, between 4 and 50 K the magnetic susceptibility decreases steeply due to paramagnetic impurities, followed by an increase between 50 and 400 K. This increase is not yet understood; explanations in terms of thermally activated charge carriers excited across an energy gap or the Bonner-Fisher model for a 1D antiferromagnetic spin-1/2 Heisenberg spin chain were proposed.[10]

The conduction mechanism of the compounds $SrNbO_{3.41}$, $SrNbO_{3.45}$, and $Sr_{0.8}La_{0.2}NbO_{3.50}$ was studied by dielectric measurements in the radio-frequency range along the *c* direction.[11] They suggest a hopping transport of charge carriers with polaronic character along *c*. The results from electron paramagnetic resonance (EPR) studies on $SrNbO_{3.41}$[10] with the magnetic field applied parallel to the *b* and *c* axis are in agreement with a variable range hopping in 1D. Furthermore, ^{93}Nb NMR measurements indicate a fluctuating quadrupole field and seem to resemble some of the characteristics of the prototypical charge-density-wave (CDW) compound $NbSe_3$.[10]

The most puzzling finding for the series $Sr_{1-y}La_yNbO_{3.50-x}$ is an extremely small energy gap at the Fermi energy for $SrNbO_{3.41}$ along the chain direction.[2] In this paper we will show that signatures of a very small energy gap are also present for the compound $SrNbO_{3.45}$. In order to understand the observed quasi-1D metallic character and the unusual properties at low temperature, we give an overview of the electronic and vibrational properties of various compounds of the series $Sr_{1-y}La_yNbO_{3.5-x}$, as obtained by optical spectroscopy in the infrared frequency range and angle-resolved photoemission spectroscopy (ARPES). We will discuss our findings for the various compounds with respect to differences in the crystal structure. Based on the comparison of our results from optics and ARPES to the dc resistivity data, we propose a possible picture for the transport mechanism and discuss the role of electron-phonon coupling in these niobate compounds.

The paper is organized as follows. The experimental details are given in Sec. II followed by the presentation of the experimental results in Sec. III. We discuss the electronic and vibrational properties of the series $Sr_{1-y}La_yNbO_{3.5-x}$ in Sec. IV and conclude with a summary of the findings in Sec. V.

II. EXPERIMENT

The investigated $SrNbO_{3.41}$, $SrNbO_{3.45}$, $SrNbO_{3.50}$, and $(Sr,Ba,Ca)_{0.8}La_{0.2}NbO_{3.50}$ single crystals with a typical size of $3\times2\times0.2$ mm^3 were grown by a floating zone melting process, and their oxygen content was determined by thermogravimetric analysis.[3] ARPES data were recorded with a Scienta ESCA-300 analyzer. The He Iα (21.22 eV) line of a standard gas discharge lamp was used. With a fixed analyzer setup the sample was rotated around one axis; the rotation angle θ determines the emission direction of the photoelectrons relative to the surface normal and thus the component *k* of the photoelectron momentum along the studied direction according to $k=\sqrt{2mE_{kin}}\sin\theta/\hbar$. The crystals, which had been oriented to $\pm1°$ by Laue diffraction before introducing them into the UHV system, were cleaved at a base pressure of 1×10^{-10} mbar and cooled down. ARPES spectra with energy resolution $\Delta E=30$ meV were recorded at temperature $T=75$ K. The sample surface quality was checked periodically by comparison of valence band features. The angular resolution of the ARPES spectra amounts to $\Delta\theta=\pm0.5°$ corresponding to $\Delta k=0.04$ Å^{-1}. The Fermi energy E_F was determined to 1 meV accuracy from the Fermi cutoff of a freshly evaporated gold film recorded immediately afterwards at the same experimental conditions.

For the reflectivity measurements the samples were carefully polished on a polishing disk using diamond paste with a grain size of 1 μm to obtain flat and shiny surfaces. Near-

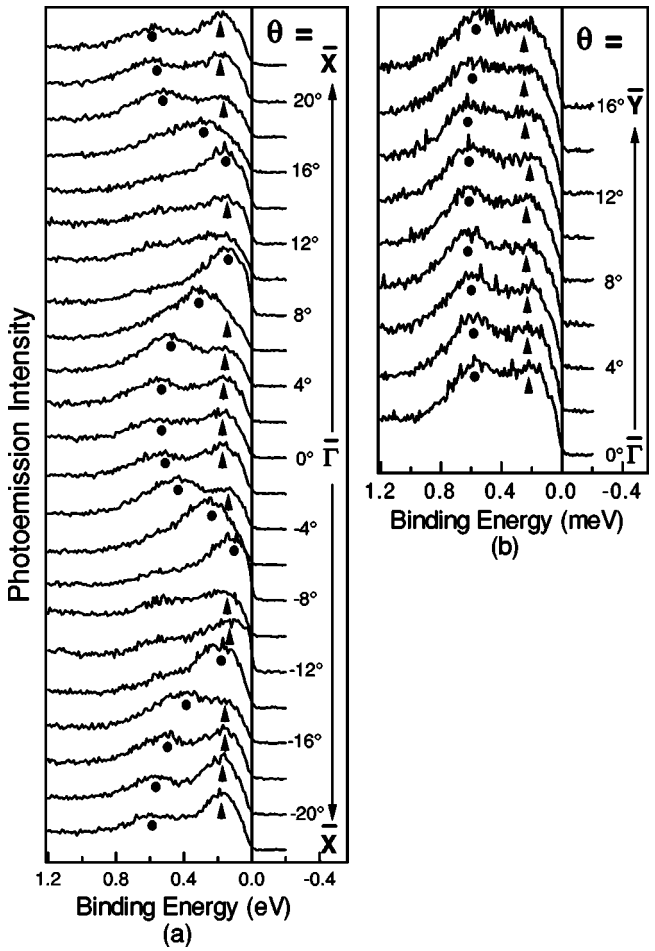

FIG. 2. ARPES spectra of $SrNbO_{3.41}$, normalized to the same total intensity, along (a) $\bar{\Gamma}-\bar{X}$ and (b) $\bar{\Gamma}-\bar{Y}$ at 75 K with $\Delta E = 30$ meV.

normal incidence reflection measurements with the electric field **E** of the incident light parallel to the a and b axes were performed for frequencies 20–10 000 cm^{-1} using a Fourier-transform spectrometer Bruker IFS 113v. The energy resolution was set to 1 cm^{-1} in the far-infrared range and to 2–4 cm^{-1} in the mid-infrared (MIR) and near-infrared range. For $SrNbO_{3.41}$, $SrNbO_{3.45}$, and $Sr_{0.8}La_{0.2}NbO_{3.50}$ the low frequency reflectivity (6–30 cm^{-1}) was studied with a quasi-optical submillimeter (submm) spectrometer[12] using backward-wave oscillators which produce monochromatic, polarized radiation continuously tunable in frequency. For $SrNbO_{3.41}$ the reflectivity spectra were extended to 34 000 cm^{-1} by utilizing a Bruker IFS 66v/S spectrometer. The use of optical cryostates enabled temperature-dependent measurements between 5 and 300 K. To obtain absolute reflectivities the spectra were divided by the reflectivity spectra of an Al mirror.

To obtain the optical conductivity $\sigma_1(\nu)$ by Kramers-Kronig analysis the reflectivity spectra $R(\nu)$ of $SrNbO_{3.41}$ and $SrNbO_{3.45}$ along the highly conducting direction were extrapolated to zero frequency according to the Hagen-Rubens relation.[13] A constant extrapolation to $\nu=0$ was chosen for the perpendicular direction. For insulating $SrNbO_{3.50}$ the value $R(0)$ for the constant low-frequency extrapolation

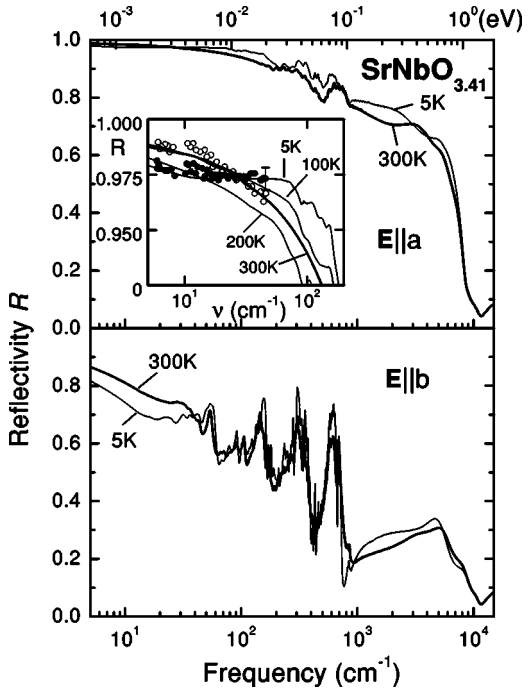

FIG. 3. Reflectivity R of $SrNbO_{3.41}$ at different temperatures for $\mathbf{E}\|a$ and $\mathbf{E}\|b$, respectively. Inset: Low-frequency reflectivity for $\mathbf{E}\|a$; open (closed) circles: submm reflectivity data at 300 K (5 K).

was calculated from the dielectric constant ϵ_1 at 1 kHz ($\epsilon_{1,a}=75, \epsilon_{1,b}=43$) (Ref. 8) according to $R(0)=[(1-\sqrt{\epsilon_1})/(1+\sqrt{\epsilon_1})]^2$. For the $Sr_{0.2}La_{0.8}NbO_{3.50}$ spectra either a Hagen-Rubens or a constant extrapolation was used, depending on the low-frequency behavior of the measured reflectivity at different temperatures. For the high-frequency extrapolation of all spectra an ν^{-4} decay was assumed.

In the case of $SrNbO_{3.45}$ the reflectivity data were supplemented by transmission measurements in the frequency range 10–20 cm^{-1} on a single crystal of thickness ≈20 μm using a Mach-Zehnder interferometer arrangement. From the independent determination of the transmission coefficient and the phase shift we were able to directly calculate the complex dielectric function $\epsilon(\nu)$ by utilizing the Fresnel equations.[12]

III. RESULTS

A. $SrNbO_{3.41}$: ARPES, optics

The k-dependent near-E_F electronic structure, as studied by ARPES, reflects the strongly anisotropic character of $SrNbO_{3.41}$ (see Fig. 2). One observes two bands near E_F, with ≈600 and ≈200 meV binding energy (BE) at the $\bar{\Gamma}$ point. Along $\bar{\Gamma}$-$\bar{X}$ [Fig. 2(a)], i.e., along the chains, the band at lower BE shows no dispersion, whereas the second band disperses strongly towards E_F, gains intensity at around $|\theta|=8°$, and loses intensity between $|\theta|=8°$ and $|\theta|=10°$ suggestive of a Fermi surface (FS) crossing. At $|\theta|\pm 14°$ the peak reappears and disperses away from E_F for higher $|\theta|$. The reappearance of the peak can be explained in terms of a 2×1 superstructure which was also observed by low energy

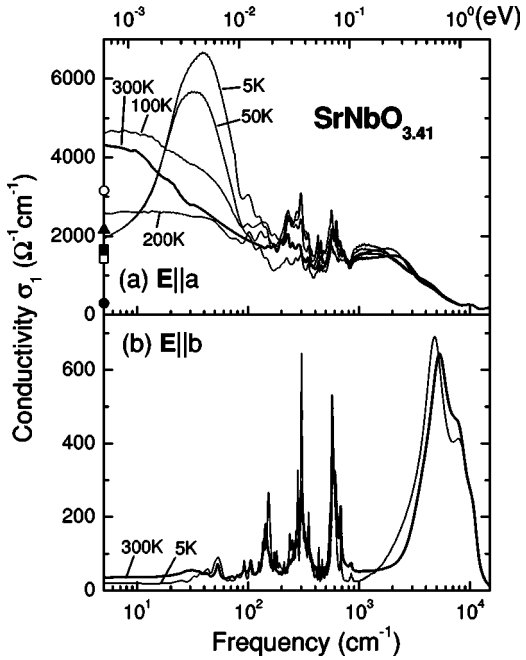

FIG. 4. Optical conductivity σ_1 of $SrNbO_{3.41}$ at different temperatures for $\mathbf{E}\|a$ and $\mathbf{E}\|b$, respectively. For $\mathbf{E}\|a$ the low-temperature peak around 40 cm^{-1} indicates excitations across a gap $2\Delta \approx 5$ meV. Also shown are the dc conductivity values for the a axis at 300 K (filled triangle), 200 K (open square), 100 K (filled square), 50 K (open circle), and 5 K (filled circle).

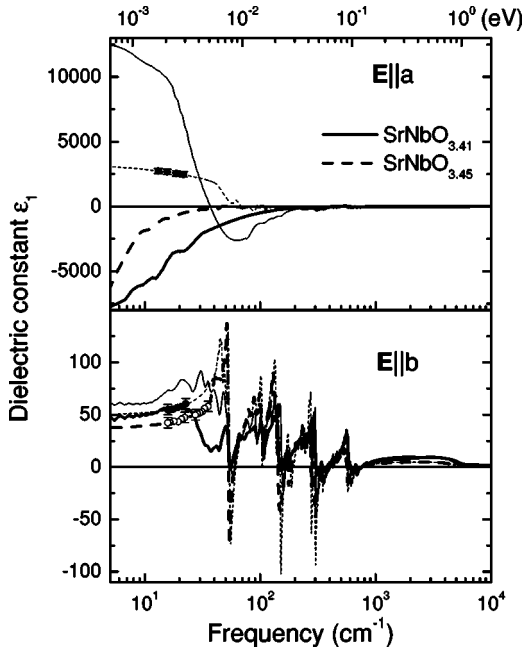

FIG. 5. Dielectric constant ϵ_1 of $SrNbO_{3.41}$ and $SrNbO_{3.45}$ at 300 K (thick lines) and 5 K (thin lines) for $\mathbf{E}\|a$ and $\mathbf{E}\|b$, respectively; open (closed) circles: data points at 300 K (5 K) directly determined by transmission measurements on a thin platelet.

electron diffraction[1,14] and neutron scattering,[15] and seems to be a characteristic property of all members of the $Sr_{1-y}La_yNbO_{3.5-x}$ series. The parabolic dispersion of the band around $\bar{\Gamma}$ and $\bar{X}$ gives an effective electron mass of $m^*/m_0 = 0.71$. Along the perpendicular direction $\bar{\Gamma}$-$\bar{Y}$ [Fig. 2(b)] both bands hardly show any dispersion.

The anisotropic character is confirmed by the strongly polarization-dependent reflectivity $R(\nu)$ shown in Fig. 3. It exhibits a plasma edge for $\mathbf{E}\|a$ and high values (≈ 1) at low frequencies indicating metallic behavior. In contrast, for $\mathbf{E}\|b$ the considerably lower reflectivity demonstrates the insulating character perpendicular to the chains. The corresponding optical conductivity σ_1 (Fig. 4) for $\mathbf{E}\|a$ consists of a Drude-like component followed by phonon modes and a relatively broad MIR band centered around 1500 cm^{-1}. A rich phonon spectrum is observed along both directions; for $\mathbf{E}\|b$ 76 lines can be resolved at RT, with the strongest modes at 144, 296, 304, 561, 572, 577, 583, 595, 603, 612, and 680 cm^{-1}. The strong double-peak structure in the $\mathbf{E}\|b$ spectrum centered around 5000 cm^{-1} can be related to interband transitions.

During cooling down considerable changes can be seen in the electronic and vibrational part of the spectra: For $\mathbf{E}\|b$ at least six new modes appear with decreasing temperature. Along the perpendicular direction, $\mathbf{E}\|a$, a strong peak appears around 40 cm^{-1} in the optical conductivity spectrum (see Fig. 4), which starts building up below 100 K. With decreasing temperature the peak shifts slightly to higher frequencies and becomes stronger. As discussed in Ref. 2 this feature can be ascribed to single-particle excitations across a gap in the electronic density of states (DOS) with 2Δ(5 K) ≈ 5 meV. The development of the peak is already indicated in the reflectivity at 5 K by the lowering and flattening of the low-frequency part of the spectrum (see inset of Fig. 3). The gap opening at low temperature strongly influences the dielectric constant $\epsilon_1(\nu \to 0)$. Assuming a simple picture of a semiconductor with an energy gap $\hbar\omega_g$ between the narrow valence and conduction band, the relation $\epsilon_1(\nu=0) \approx \omega_g^{-2}$ is expected to hold.[13] This explains the measured spectrum $\epsilon_1(\nu)$ of $SrNbO_{3.41}$ for $\mathbf{E}\|a$ (Fig. 5), where at 5 K high positive values are found for $\nu \to 0$. In contrast, at 300 K $\epsilon_1(\nu \to 0)$ is negative as expected for a metal. These findings confirm the high-resolution ARPES data, which show a gap between the leading edge midpoint of the spectrum and E_F of $\Delta(25\text{ K}) \approx 4$ meV for $\bar{\Gamma}-\bar{X}$.[2] The gap opening as observed by optics and ARPES along the chain direction is in agreement with the dc resistivity data along the a direction, although there the upturn occurs at a lower temperature ($\approx$50 K) than the development of the low-frequency peak in the optical conductivity (below 100 K), as was already pointed out in Ref. 2. In Fig. 4 we also included the dc conductivity results;[3] above 50 K the dc values are obviously lower than the optical conductivity values at 5 cm^{-1}. This suggests that the optical conductivity σ_1 cannot be described by a simple Drude-type behavior. Fitting the $\sigma_1(\omega)$ spectra with the Drude-Lorentz model indeed shows that a fit of reasonable quality (not shown) requires the introduction of two Drude peaks, e.g., with $\sigma_{1,1}(\omega \to 0) = 2006\ \Omega^{-1}\,cm^{-1}$ and $\sigma_{1,2}(\omega \to 0) = 2356\ \Omega^{-1}\,cm^{-1}$ at 300 K, which is in good agreement with the corresponding dc conductivity value.

B. $SrNbO_{3.50}$: Optics

The reflectivity spectra of $SrNbO_{3.50}$ (insets of Fig. 6) are significantly different from those of $SrNbO_{3.41}$. The overall

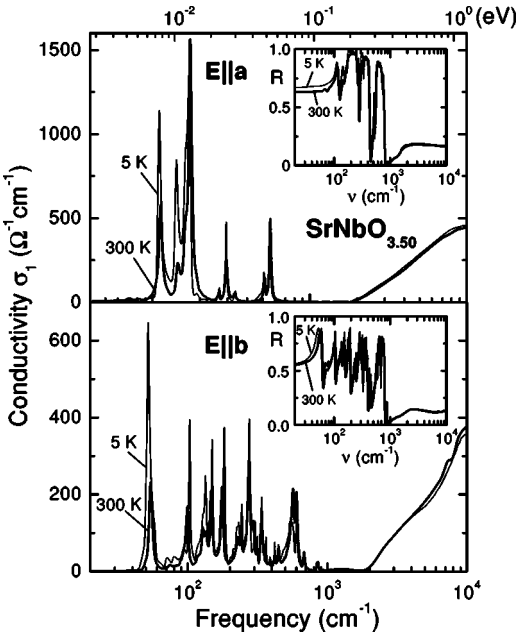

FIG. 6. Optical conductivity σ_1 of $SrNbO_{3.50}$ at 300 and 5 K for $\mathbf{E}\|a$ and $\mathbf{E}\|b$, respectively. Insets: Reflectivity R used for Kramers-Kronig analysis.

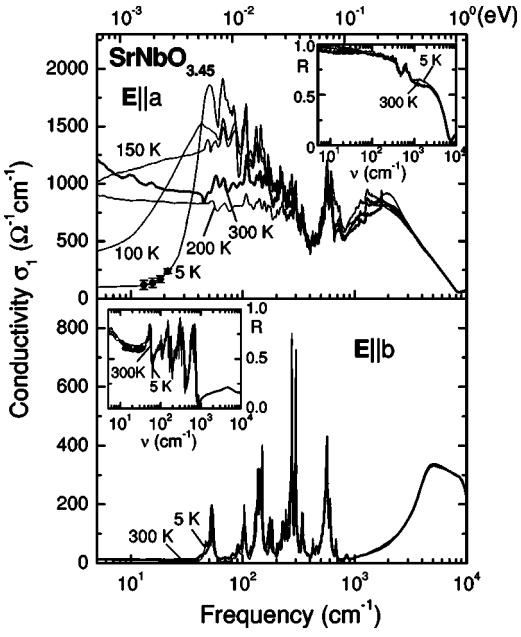

FIG. 7. Optical conductivity σ_1 of $SrNbO_{3.45}$ at different temperatures for $\mathbf{E}\|a$ and $\mathbf{E}\|b$, respectively; closed circles: data points directly determined by transmission measurements on a thin platelet. For $\mathbf{E}\|a$ the low-temperature peak in σ_1 with its maximum around 60 cm^{-1} indicates excitations across a gap $2\Delta \approx 7$ meV. Insets: Reflectivity R used for Kramers-Kronig analysis; open (closed) circles: submm reflectivity data at 300 K (5 K).

low reflectivity for both polarization directions is in accordance with the insulating nature of the material. The nonconducting character is also illustrated in the optical conductivity spectra (Fig. 6) which do not contain electronic excitations in the low-frequency range (the onset of interband transitions is around 2000 cm^{-1} for both polarizations) but only vibrational excitations. Perpendicular to the chains, i.e., for $\mathbf{E}\|b$, a rich phonon spectrum is found. At RT one can resolve 24 infrared active modes for $\mathbf{E}\|b$, with the strongest around 54, 100, 147, 176, 275, 295, 338, 567, and 601 cm^{-1}, and 12 modes for $\mathbf{E}\|b$, the strongest being around 112, 173, 295, and 561 cm^{-1}. A qualitative assignment of the phonon modes is given in the discussion. The mode around 54 cm^{-1} for $\mathbf{E}\|b$ is close to the soft mode found by Raman scattering experiments[16] which is related to the ferroelectric transition at 1615 K. It is expected to be infrared active, and indeed was already observed in earlier reflectivity and transmission studies.[17] During cooling down additional modes appear in agreement with the results of Ref. 17, and at 5 K there are altogether 24 and 51 modes resolved for $\mathbf{E}\|a$ and $\mathbf{E}\|b$, respectively. The number of observed modes at RT and 5 K is lower than expected from the factor group analysis;[17] the missing modes might be either masked by the other contributions or too weak to be resolved.

C. $SrNbO_{3.45}$: Optics

Previous ARPES measurements[1,18] on $SrNbO_{3.45}$ revealed a quasi-1D band structure near E_F similar to that of $SrNbO_{3.41}$. Also the optical response shown in Fig. 7 clearly demonstrates strong similarities in the electronic properties between the two compounds: The $\mathbf{E}\|a$ reflectivity R at RT is high and almost 1 at low frequencies and shows a pseudo plasma edge, whereas for $\mathbf{E}\|b$ the overall reflectivity is low and no plasma edge is found. Correspondingly, for $\mathbf{E}\|a$ the optical conductivity contains a Drude-like peak due to itinerant electrons which is superimposed by vibrational modes between 50 and 800 cm^{-1}, followed by a pronounced MIR band centered around 2000 cm^{-1} with a vibrational fine structure. In contrast, for $\mathbf{E}\|b$ no Drude peak is observed in $\sigma_1(\nu)$ but a large number of vibrational excitations up to 900 cm^{-1} followed by interband transitions above $\approx$2000 cm^{-1}. Thus, also $SrNbO_{3.45}$ shows a quasi-1D metallic character at RT, with a metal-like behavior along the chains and an insulating behavior along the perpendicular direction.

The temperature dependence of the low-frequency optical properties along the chains agrees qualitatively with the dc resistivity,[19] being almost temperature-independent between 300 and $\approx$100 K and increases below 100 K with decreasing temperature. Substantial changes occur in the low-frequency ($\leqslant$50 cm^{-1}) optical response of $SrNbO_{3.45}$ at low temperatures ($<$100 K): One observes a lowering and flattening of the reflectivity (see the inset of Fig. 7) which signals the development of a new excitation. According to the optical conductivity (Fig. 7) between 0 and 400 cm^{-1} a redistribution of spectral weight from low to high frequencies occurs for temperatures below 150 K, resulting in the development of a relatively broad and asymmetric peak, which has a maximum around 60 cm^{-1} ($\approx$7 meV) and is superimposed by a large number of phonon excitations. The peak intensity increases with decreasing temperature. One can ascribe the development of the low-frequency peak to the opening of an energy gap with decreasing temperature. The presence of a

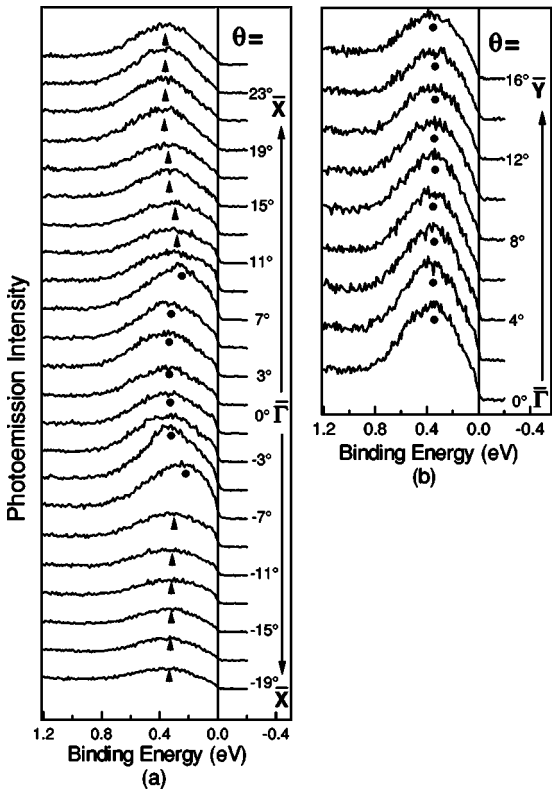

FIG. 8. ARPES spectra of $Sr_{0.8}La_{0.2}NbO_{3.50}$ along (a) $\bar{\Gamma}-\bar{X}$ and (b) $\bar{\Gamma}-\bar{Y}$ at 75 K with $\Delta E=30$ meV.

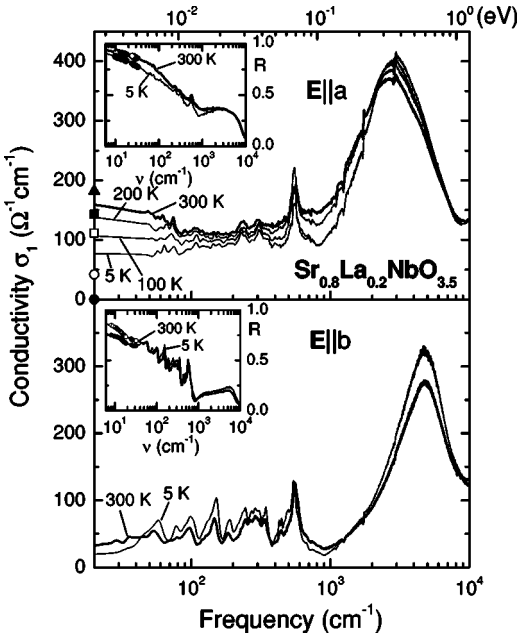

FIG. 9. Optical conductivity σ_1 of $Sr_{0.8}La_{0.2}NbO_{3.50}$ at different temperatures for $\mathbf{E}\|a$ and $\mathbf{E}\|b$, respectively. Also shown are the dc conductivity values for the a axis at 300 K (filled triangle), 200 K (open square), 100 K (filled square), 50 K (open circle), and 5 K (filled circle). Insets: Reflectivity R used for Kramers-Kronig analysis; open (closed) circles: submm reflectivity data at 300 K (5 K).

small gap at low temperature is also indicated by the high values of the corresponding dielectric constant ϵ_1 at 5 K for $\nu\rightarrow 0$ (Fig. 5), as was discussed for $SrNbO_{3.41}$ in Sec. III A. In summary, $SrNbO_{3.45}$ resembles the electronic properties of $SrNbO_{3.41}$ by showing both a quasi-1D metallic character and the opening of an energy gap of only a few milli-electron-volts size below 150 K.

D. $Sr_{0.8}La_{0.2}NbO_{3.50}$: ARPES, optics

The electronic properties of $Sr_{0.8}La_{0.2}NbO_{3.50}$ near E_F were studied by ARPES along the two high-symmetry lines $\bar{\Gamma}-\bar{X}$ and $\bar{\Gamma}-\bar{Y}$; the results are depicted in Fig. 8. At the $\bar{\Gamma}$ point we observe a broad peak around 350 meV BE. Along $\bar{\Gamma}-\bar{X}$ the peak slowly disperses towards E_F accompanied by an intensity increase and between $|\theta|=7°$ and $|\theta|=9°$ the intensity of the peak slightly drops; at higher emission angles a broad peak is still visible with almost constant BE ($\approx$350 meV). Along $\bar{\Gamma}-\bar{Y}$ no dispersion of the broad peak is observed. Along both directions and for all emission angles the overall photoelectron intensity near E_F is quite low. We also studied the ARPES spectra for $Sr_{0.7}La_{0.2}Ba_{0.1}NbO_{3.50}$ and $Sr_{0.6}La_{0.2}Ca_{0.2}NbO_{3.50}$ (not shown), having the same nominal carrier density as $Sr_{0.8}La_{0.2}NbO_{3.50}$ (see Table I): For these two compounds the dispersion of the broad peak along $\bar{\Gamma}-\bar{X}$ for $|\theta|\leqslant 7°$ is even less pronounced.[14] The results for the $(Sr,Ba,Ca)_{0.8}La_{0.2}NbO_{3.50}$ suggest that there are two near-E_F bands with similar BEs: One band is almost dispersionless along both $\bar{\Gamma}-\bar{X}$ and $\bar{\Gamma}-\bar{Y}$; the second band has a parabolike dispersion, although very weak, along $\bar{\Gamma}-\bar{X}$ with an intensity drop near E_F suggestive of a FS crossing, and is dispersionless along $\bar{\Gamma}-\bar{Y}$. To some extent the band dispersions of $Sr_{0.8}La_{0.2}NbO_{3.50}$ thus resemble those of $SrNbO_{3.41}$ (see Fig. 2). However, compared to $SrNbO_{3.41}$ the dispersion along $\bar{\Gamma}-\bar{X}$ is much weaker, i.e., the quasi-1D character of the band structure is less developed.

Further insight was gained by temperature-dependent reflectivity measurements for $\mathbf{E}\|a,b$ (see Fig. 9). For the polarization $\mathbf{E}\|b$ the overall low reflectivity and the absence of a Drude component in $\sigma_1(\nu)$ demonstrate the insulating character of the material perpendicular to the chains. For $\mathbf{E}\|a$ the reflectivity at RT is metal like with relatively high values at low frequencies, decreases for higher frequencies, and finally drops rapidly above 6000 cm^{-1}. The corresponding optical conductivity shows a very weak Drude-like contribution and a pronounced MIR absorption peak around 3000 cm^{-1}. Between 300 and 50 K the low-frequency optical conductivity is in reasonable agreement with the dc conductivity,[3] but at 5 K it is higher than the dc value. The overall optical response of $Sr_{0.8}La_{0.2}NbO_{3.50}$ is similar to that of $SrNbO_{3.41}$ (see Fig. 4) and $SrNbO_{3.45}$ (see Fig. 7), but there are important differences. The overall reflectivity of $Sr_{0.8}La_{0.2}NbO_{3.50}$ along the chains is lower in the far-infrared range and the plasma edge is hardly developed; both findings indicate only weak metallic character. Thus, the optical conductivity of $Sr_{0.8}La_{0.2}NbO_{3.50}$ for $\mathbf{E}\|a$ contains a much weaker Drude-like term. Importantly, with decreasing temperature the

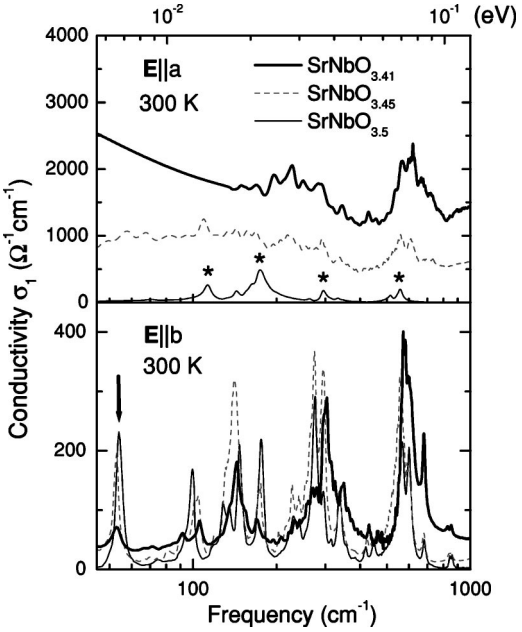

FIG. 10. Optical conductivity σ_1 of $SrNbO_{3.50}$, $SrNbO_{3.45}$, and $SrNbO_{3.41}$ at RT for $\mathbf{E}\|a$ and $\mathbf{E}\|b$, respectively. The asterisks mark the phonon lines of $SrNbO_{3.50}$ for $\mathbf{E}\|a$ which survive in the conducting compounds. The arrow indicates the ferroelectric soft mode of $SrNbO_{3.50}$.

development of a low-frequency peak is not observed, in contrast to what is found for $SrNbO_{3.41}$ and $SrNbO_{3.45}$ (see Figs. 4 and 7).

IV. DISCUSSION

According to the experimental results, the electronic properties of the $SrNbO_{3.50-x}$ compounds strongly depend on the oxygen content, which not only determines the crystal structure, but also the number of conduction electrons in the material (see Table I). To illustrate these differences we plot in Fig. 10 the optical conductivity at RT for the three compositions $SrNbO_{3.41}$, $SrNbO_{3.45}$, and $SrNbO_{3.50}$ for $\mathbf{E}\|a,b$. A contribution of itinerant electrons appears in the $\mathbf{E}\|a$ spectra: A Drude peak is observed for $SrNbO_{3.45}$, which is even more pronounced for $SrNbO_{3.41}$ in full agreement with the higher density of conduction electrons for the latter compound, while the absence of a Drude peak for $SrNbO_{3.50}$ accounts for its insulating character.

Despite their layered crystal structure, $SrNbO_{3.45}$ and $SrNbO_{3.41}$ show a pronounced quasi-1D metallic character which can be related to the chain-like arrangement of NbO_6 octahedra along the a axis. A more detailed picture is provided by band structure calculations in the local density approximation (LDA) for $SrNbO_{3.41}$.[1,20] The predominant contribution to the DOS near E_F is attributed to the Nb site in the middle of the slab, while the other two[21] Nb sites contribute considerably less [see Fig. 6(a) in Ref. 20]. The corresponding NbO_6 octahedra in the middle of the slabs (marked by thick lines in Fig. 1) are the least distorted ones, with the Nb atoms located right in the center of the octahedra; for all other octahedra the Nb atoms are considerably shifted away

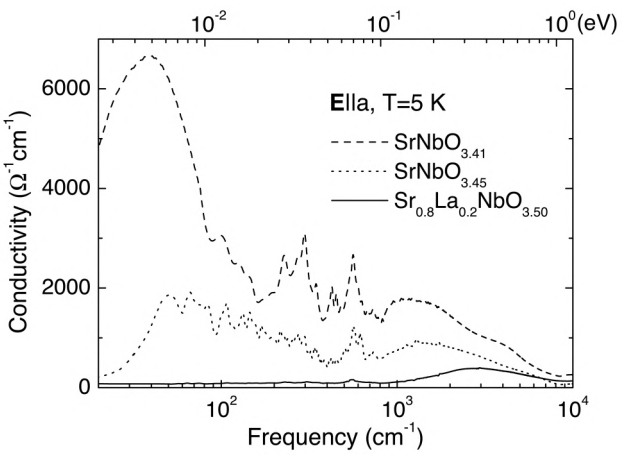

FIG. 11. Optical conductivity σ_1 of $SrNbO_{3.41}$, $SrNbO_{3.45}$, and $Sr_{0.8}La_{0.2}NbO_{3.50}$ at 5 K for $\mathbf{E}\|a$.

from the central octahedral position. The quasi-1D metallic character is thus related to the central chains of least distorted octahedra in the middle of the slabs. The influence of the central octahedral chains on the electronic characteristics is illustrated by the experimental results of $Sr_{0.8}La_{0.2}NbO_{3.50}$ compared to those of $SrNbO_{3.41}$. Both compounds nominally contain the same density of Nb 4d conduction electrons (see Table I). However, in $Sr_{0.8}La_{0.2}NbO_{3.50}$ the slabs are only *four* octahedra wide, i.e., the central chains are missing. According to the resistivity[3] and optical results presented here, this compound shows a much weaker metallic behavior compared to $SrNbO_{3.41}$, and the quasi-1D character of its band structure, as observed by ARPES, has almost vanished. This is in agreement with the absence of a gap opening for $Sr_{0.8}La_{0.2}NbO_{3.50}$ along the chains (see Fig. 11). The intensity of the weak Drude peak observed in the RT optical conductivity for $\mathbf{E}\|a$ has decreased at 5 K, but a low-frequency peak has not developed, in contrast to what is found for $SrNbO_{3.41}$ and $SrNbO_{3.45}$. All these experimental findings show that the quasi-1D metallic character and the related gap opening observed for $SrNbO_{3.41}$ and $SrNbO_{3.45}$ are indeed linked to the central octahedral chains.

The compounds $SrNbO_{3.50}$, $SrNbO_{3.45}$, and $SrNbO_{3.41}$ have a complex crystal structure and thus exhibit rich phonon spectra for both polarization directions (see Fig. 10). For $\mathbf{E}\|a$ the main groups of phonon modes observed for $SrNbO_{3.50}$, which are centered around 110, 170, 300, and 540 cm^{-1} and marked by asterisks in Fig. 10, survive in the conducting members, with only small frequency shifts and a masking due to the contribution of itinerant electrons. The similarities in the vibrational properties are more obvious for the polarization direction perpendicular to the chains, $\mathbf{E}\|b$, since no Drude contribution is present. The main groups of phonon lines, centered around 53, 100, 150, 290, and 600 cm^{-1}, are present in all three compounds. A qualitative assignment to the lattice dynamics can be achieved by a comparison with other niobium oxides with a similar network of corner-sharing NbO_6 octahedra. The high-frequency infrared-active modes of $KNbO_3$ ($NaNbO_3$) were assigned to the internal modes of NbO_6 octahedra, namely the 660 (675)

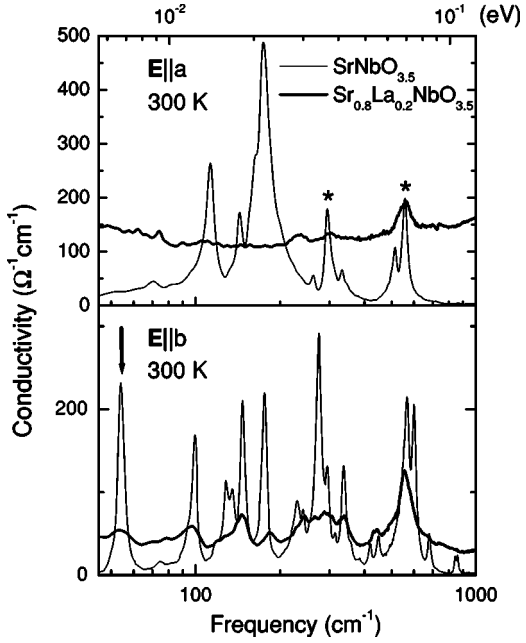

FIG. 12. Optical conductivity σ_1 of $SrNbO_{3.50}$ and $Sr_{0.8}La_{0.2}NbO_{3.50}$ at RT for $\mathbf{E}\|a$ and $\mathbf{E}\|b$, respectively. The asterisks mark the phonon lines of $SrNbO_{3.50}$ for $\mathbf{E}\|a$ which survive in the conducting compound. The arrow indicates the ferroelectric soft mode of $SrNbO_{3.50}$.

and 550 (510) cm^{-1} modes to the stretching modes and the 375 (375) cm^{-1} mode to the bending mode.[22] This is in agreement with later Raman and infrared measurements on $LiNbO_3$ and $Ba_2NaNb_5O_{15}$.[23] The lower-frequency lines ($\nu < 200\ cm^{-1}$) were assigned to translational modes of the cations.[23] The influence of La doping on the optical properties is illustrated in Fig. 12 where we plot the conductivity spectra of $SrNbO_{3.50}$ and $Sr_{0.8}La_{0.2}NbO_{3.50}$. For $\mathbf{E}\|a$ an electronic background related to itinerant carriers in the $Sr_{0.8}La_{0.2}NbO_{3.50}$ spectrum is visible. Two of the main groups of phonon modes of $SrNbO_{3.50}$ (marked by asterisks) are also present in the (weakly) conducting material, but they are broader and strongly damped. Interestingly, the relatively strong modes observed in $SrNbO_{3.50}$ around 110 and 170 cm^{-1} appear to be completely suppressed in $Sr_{0.8}La_{0.2}NbO_{3.50}$, indicating a strong damping of the cation translational modes by partial substitution of Sr by La. Along the b direction the similarities in the vibrational properties are also obvious. In particular, the mode around 54 cm^{-1} for $\mathbf{E}\|b$, indicated by an arrow in Figs. 10 and 12 is present in all four compounds discussed here. For $SrNbO_{3.50}$ this mode was assigned to the soft mode of the ferroelectric phase transition at 1615 K, based on Raman scattering experiments.[16] It was also observed in recent optical measurements and related to NbO_6 octahedra tiltings.[17] In agreement with Ref. 17, this soft mode is temperature independent between 300 and 100 K and shifts to higher frequencies below 100 K. The precise temperature dependence is, however, difficult to determine due to the overlap with another mode which appears around 50 cm^{-1} at $\approx$100 K during cooling down.

Finally, we want to discuss the puzzling electronic properties of the conducting members of the present niobate series at low temperature, in particular the opening of an energy gap at E_F found for $SrNbO_{3.41}$ and $SrNbO_{3.45}$. Several aspects make an explanation of the gap opening in terms of a Peierls-type scenario most likely: (i) The FS nesting[1] could drive the lattice towards a Peierls distortion; (ii) the shadow band observed for $SrNbO_{3.41}$ in ARPES[2] would be consistent with a superstructure with wave vector $q=2k_F$;[24] and (iii) the appearance of phonon lines with decreasing temperature suggests a structural phase transition such as a Peierls instability. However, there remain some inconsistencies within a Peierls scenario: In contrast to what is expected for CDW formation, no sharp anomaly is found in the dc resistivity; neither do thermal expansion measurements[25] show indications of a structural phase transition. Furthermore, an estimate of the mean-field transition temperature based on the observed gap size is not compatible with the temperature development of the dc resistivity and optical conductivity.[2]

Further open issues are the transport mechanism in $SrNbO_{3.41}$ and $SrNbO_{3.45}$ along the chain direction and the closely related temperature dependence of the dc resistivity ρ_a, showing different regimes. The strong upturn of ρ_a below 50 K with cooling down can be explained by the opening of a gap, in agreement with ARPES and optics. The temperature dependence above 50 K may be due to contributions of quasiparticles with different characteristics. While the metallic temperature dependence between 50 and 130 K suggests a band-like motion of electrons, above 130 K the hopping of more localized charge carriers appears to dominate. A possible mechanism for the localization/trapping of charge carriers could be strong electron-phonon coupling, which might also explain the observation of a pronounced MIR absorption band in the optical conductivity along the chain direction (see Figs. 4 and 7). Similar absorption bands in related quasi-1D metallic compounds were recently interpreted in terms of excitations of polaronic quasiparticles.[26,27] Further spectroscopic information, e.g., from temperature-dependent ARPES measurements, is needed to clarify a possible polaron formation in the studied niobates.

In conclusion, we determined the electronic and vibrational properties of the perovskite-related compounds $Sr_{1-y}La_yNbO_{3.5-x}$ and related the results to their crystal structure. A possible transport mechanism of $SrNbO_{3.41}$ and $SrNbO_{3.45}$ was discussed and the importance of electron-phonon coupling in these systems suggested, possibly leading to polaron formation. To explain the low-temperature behavior a Peierls picture appears to be the most appropriate, but is insufficient to describe all the findings. An important aspect might be the close structural affinity of the quasi-1D metals $SrNbO_{3.41}$ and $SrNbO_{3.45}$ to the ferroelectric $SrNbO_{3.50}$: $SrNbO_{3.41}$ [and the ($n=5$) slabs in $SrNbO_{3.45}$] contains the same structural building blocks as $SrNbO_{3.50}$, but with additional chains of basically *undistorted* NbO_6 octahedra inserted in the center of the slabs. Ferroelectric $SrNbO_{3.50}$ shows relatively high values of the static dielectric constant ϵ_1 at RT ($\epsilon_{1,a}=75$, $\epsilon_{1b}=43$, and $\epsilon_{1,c}=46$)[8] indicating highly polarizable structural units. A further important result is the observation of the phonon mode at 54 cm^{-1} in the $\mathbf{E}\|b$ conductivity spectra of all present niobate compounds (see Figs. 10 and 12), which for $SrNbO_{3.50}$ can be assigned to the

ferroelectric soft mode. Since the soft modes in ferroelectrics in general lead to electrical polarization, the presence of the 54 cm^{-1} mode in $SrNbO_{3.41}$ and $SrNbO_{3.45}$ indicates a polarizability of their lattices. The highly conducting channels of octahedra in the middle of the slabs, which are responsible for the 1D metallic transport, can thus be viewed as embedded in a highly polarizable medium, and a certain influence of this medium on the electronic properties of the chains is conceivable. This picture is, however, speculative since to our knowledge a 1D model taking into account such a polarizable medium surrounding the conducting entities does not exist.

V. SUMMARY

By angle-resolved photoemission spectroscopy and polarization-dependent reflectivity measurements in the infrared we studied the electronic and vibrational properties of several members of the series $Sr_{1-y}La_yNbO_{3.50-x}$ $(0 \leqslant x \leqslant 0.1)$ along and perpendicular to the chains of NbO_6 octahedra. $SrNbO_{3.50}$ is a ferroelectric insulator with a rich phonon spectrum for both polarization directions $\mathbf{E} \| a,b$. At room temperature the compounds $SrNbO_{3.41}$ and $SrNbO_{3.45}$ exhibit a metallic behavior with a strongly dispersing band along the chains ($\mathbf{E} \| a$) and an insulating, nondispersive character in the perpendicular direction ($\mathbf{E} \| b$); they are thus quasi-1D metals. Despite the similar carrier density, for $Sr_{0.8}La_{0.2}NbO_{3.50}$ the quasi-1D metallic character is much less developed. Based on a comparison between the experimental results of $SrNbO_{3.41}$, $SrNbO_{3.45}$, and $Sr_{0.8}La_{0.2}NbO_{3.50}$ the quasi-1D metallic character observed in this series can be related to the central chains of least distorted octahedra located in the middle of the slabs. This is in full agreement with the results from LDA band structure calculations. We propose a possible transport mechanism for the compounds $SrNbO_{3.41}$ and $SrNbO_{3.45}$, with a bandlike contribution of mobile carriers and a contribution due to the hopping motion of more localized charges dominating above 130 K. At low temperature the opening of an extremely small energy gap at E_F is observed for $SrNbO_{3.41}$ and $SrNbO_{3.45}$ along the chain direction, which might be related to a Peierls-type instability, with electron-phonon coupling as the driving mechanism. However, not all findings can be explained within a Peierls picture, and we speculate that the highly polarizable structural units surrounding the conducting channels might have an appreciable influence.

ACKNOWLEDGMENTS

We are grateful to L. Perfetti, C. Rojas, and I. Vobornik for valuable technical help. We thank H. Winter for fruitful discussions. Financial support by the DAAD, the BMBF (Project No. 13N6918/1), and the Deutsche Forschungsgemeinschaft is gratefully acknowledged.

*Present address: General Physics Institute, Russian Academy of Sciences, Vavilov 38, Moscow 117942, Russia.

[1] C. A. Kuntscher, S. Gerhold, N. Nücker, T. R. Cummins, D.-H. Lu, S. Schuppler, C. S. Gopinath, F. Lichtenberg, J. Mannhart, and K.-P. Bohnen, Phys. Rev. B **61**, 1876 (2000).

[2] C. A. Kuntscher, S. Schuppler, P. Haas, B. Gorshunov, M. Dressel, M. Grioni, F. Lichtenberg, A. Herrnberger, F. Mayr, and J. Mannhart, Phys. Rev. Lett. **89**, 236403 (2002).

[3] F. Lichtenberg, A. Herrnberger, K. Wiedenmann, and J. Mannhart, Prog. Solid State Chem. **29**, 1 (2001).

[4] S. C. Abrahams, H. W. Schmalle, T. Williams, A. Reller, F. Lichtenberg, D. Widmer, J. G. Bednorz, R. Spreiter, Ch. Bosshard, and P. Günter, Acta Crystallogr., Sect. B: Struct. Sci. **B54**, 399 (1998).

[5] T. Williams, F. Lichtenberg, D. Widmer, J. G. Bednorz, and A. Reller, J. Solid State Chem. **103**, 375 (1993).

[6] J. G. Bednorz, K. H. Wachtmann, R. Broom, and D. Ariosa, in *High-T_c Superconductivity 1996: Ten Years after the Discovery*, edited by E. Kaldis, E. Liarokapis, and K. A. Müller (Kluwer, Dordrecht, 1997).

[7] S. Nanamatsu, M. Kimura, K. Doi, and M. Takahashi, J. Phys. Soc. Jpn. **30**, 300 (1971);

[8] S. Nanamatsu, M. Kimura, and T. Kawamura, J. Phys. Soc. Jpn. **38**, 817 (1975).

[9] K. Ohi, M. Kimura, H. Ishida, and H. Kakinuma, J. Phys. Soc. Jpn. **46**, 1387 (1979).

[10] J.-E. Weber, C. Kegler, N. Büttgen, H.-A. Krug von Nidda, A. Loidl, and F. Lichtenberg, Phys. Rev. B **64**, 235414 (2001).

[11] V. Bobnar, P. Lunkenheimer, J. Hemberger, A. Loidl, F. Lichtenberg, and J. Mannhart, Phys. Rev. B **65**, 155115 (2002).

[12] G. V. Kozlov and A. A. Volkov, in *Millimeter and Submillimeter Wave Spectroscopy of Solids*, edited by G. Grüner (Springer, Berlin, 1998).

[13] M. Dressel and G. Grüner, *Electrodynamics in Solids: Optical Properties of Electrons in Matter* (Cambridge University Press, Cambridge, 2002).

[14] C. A. Kuntscher, Ph.D. thesis, Universität Karlsruhe (Cuvillier Verlag, Göttingen, 2000).

[15] L. Pintschovius (unpublished).

[16] K. Ohi and S. Kojima, Jpn. J. Appl. Phys., Part 1 **24**, 817 (1985).

[17] E. Buixaderas, S. Kamba, and J. Petzelt, J. Phys.: Condens. Matter **13**, 2823 (2001).

[18] D. H. Lu, C. S. Gopinath, M. Schmidt, T. R. Cummins, N. Nücker, S. Schuppler, and F. Lichtenberg, Physica C **282–287**, 995 (1997).

[19] No dc resistivity data are available for $SrNbO_{3.45}$, but it is expected to be qualitatively similar to those of $Sr_{0.96}Ba_{0.04}NbO_{3.45}$ which has the same crystal structure (see Ref. 3) and, within an ionic picture, the same electron doping as $SrNbO_{3.45}$.

[20] H. Winter, S. Schuppler, and C. A. Kuntscher, J. Phys.: Condens. Matter **12**, 1735 (2000).

[21] There are three inequivalent Nb sites per unit cell in $SrNbO_{3.41}$, as was illustrated in Ref. 20.

[22] J. T. Last, Phys. Rev. **105**, 1740 (1957).

[23] S. D. Ross, J. Phys. C **3**, 1785 (1970).

[24] J. Voit, L. Perfetti, F. Zwick, H. Berger, G. Margaritondo, G. Grüner, H. Höchst, and M. Grioni, Science **290**, 501 (2000).
[25] P. Nagel, V. Pasler, and C. Meingast (unpublished).
[26] C. Presura, M. Popinciuc, P. H. M. van Loosdrecht, D. van der Marel, M. Mostovoy, T. Yamauchi, and Y. Ueda, Phys. Rev. Lett. **90**, 026402 (2003).
[27] C. A. Kuntscher, D. van der Marel, M. Dressel, F. Lichtenberg, and J. Mannhart, Phys. Rev. B **67**, 035105 (2003).